

Article

# The Supramolecular Organogel Formed by Self-Assembly of Ursolic Acid Appended with Aromatic Rings

Jinrong Lu, Jinshan Hu, Yinghua Liang and Wenquan Cui \*

College of Chemical Engineering, Hebei Key Laboratory for Environment Photocatalytic and Electrocatalytic Materials, North China University of Science and Technology, Tangshan 063210, China; lujinrong@ncst.edu.cn (J.L.); jinshanhu@ncst.edu.cn (J.H.); liangyh@ncst.edu.cn (Y.L.)

\* Correspondence: wqcui@ncst.edu.cn

Received: 23 January 2019; Accepted: 14 February 2019; Published: 18 February 2019



**Abstract:** Ursolic acid (UA) as a natural ursane-triterpenoid has rich pharmacological activities. We have found that it possesses aggregation properties and could self-assemble into organogels. Based on the aggregation property of ursolic acid in suitable solvents, its derivative appended with aromatic rings by amide groups was synthesized. The property of self-assembly into organogel was studied in this paper. The results revealed that this derivative could form supramolecular gel in halogenated benzene and also gelate chloroform in the presence of toluene or *p*-xylene. By Fourier-transform infrared spectra (FT-IR) and variable temperature proton nuclear magnetic resonance ( $^1\text{H}$  NMR), it was proved that intermolecular hydrogen bonding and  $\pi$ - $\pi$  stacking interaction were the primary driving forces for the aggregation to form organogel.

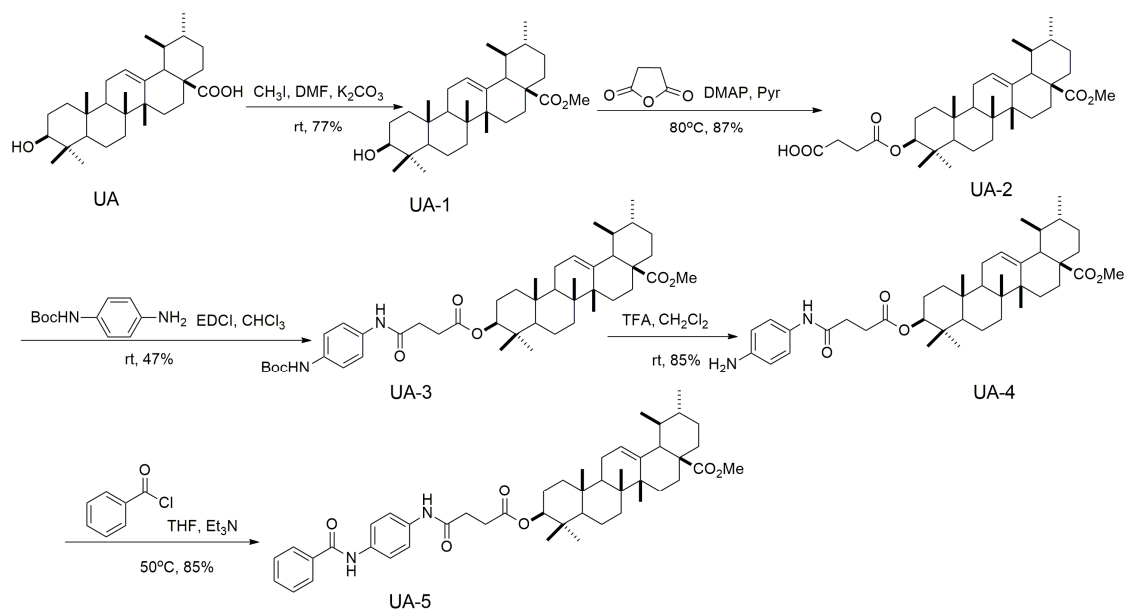
**Keywords:** ursolic acid; derivative; supramolecular organogel

## 1. Introduction

Supramolecular gel formed by the self-assembly of some organic molecules into a three-dimensional network which can trap solvent molecules is an attractive part of supramolecular chemistry [1,2]. Small organic molecules called gelators constitute the architectures of supramolecular gels. Specific functions and properties of gels can be achieved by designing gelators between which the interactions such as hydrogen bonding,  $\pi$ - $\pi$  stacking interaction, van der Waals forces, charge-transfer and electrostatic interactions, which drive the formation of their architectures [3–5]. Due to the ability of bottom-up self-assembly through the above interactions, biomolecules such as steroids, nucleobases and amino acids are attractive candidates to construct supramolecular gels through simple chemical modification [6–9]. Therefore, imitating and modifying natural products as well-defined building blocks for self-assembly could minimize tedious synthesis work.

Among natural products, triterpenoids characterized by biocompatibility, rigid chiral skeletons and chemical reaction sites were also found to have strong aggregation trends in suitable solvents [10]. For example, lupine-triterpenoid arjunolic acid [11,12], oleanane-triterpenoid glycyrrhetic acid [13–18], betulinic acid [19,20] and oleanolic acid [21,22] could all aggregate in suitable solvents and form supramolecular gel. Based on their aggregation properties, some functional groups which could provide additional non-covalent interactions could be grafted into triterpenoid skeletons to develop supramolecular self-assembly systems. So, a series of self-assembly structures based on their functional derivatives have been constructed during the last decades [23].

Ursolic acid (UA) (Scheme 1) in the form of ursane-triterpenoids has demonstrated anticancer, anti-inflammatory, antioxidant and hypotensive pharmacological activities [24–26]. Hence, it is widely used in medicine and natural whitening cosmetics. The aggregation property of unmodified ursolic acid was first reported by the authors in 2016 [27]. It was illustrated that ursolic acid could self-assemble into organogels in bromobenzene and some alcoholic solvents, which proved the aggregation property of the rigid chiral skeleton of ursolic acid. Hypothetically, designing derivatives of ursolic acid conjugated with functional groups which could provide non-covalent interactions may develop functional supramolecular assemblies based on ursolic acid. However, there are few studies on the self-assembly properties of its functional molecules, which are important for their applications. As we know,  $\pi$ - $\pi$  stacking and hydrogen bonding are the more effective and commonly used non-covalent interactions. Moreover,  $\pi$ - $\pi$  stacking of aromatic rings can reduce steric repulsion [28,29]. Herein, in order to develop the self-assembly system based on ursolic acid, the derivative UA-5 (Scheme 1) of ursolic acid appended with aromatic rings was designed. Benzene rings were connected to UA by amide groups which could provide hydrogen bonding interactions. The self-assembly properties were studied, and the results demonstrated that UA could self-assemble into nanofibers and form a 3D network in a mixture of chloroform and aromatic solvents. It was proved that the driving forces were a combination of hydrogen bonding,  $\pi$ - $\pi$  stacking and van der Waals forces.



**Scheme 1.** The synthetic route of compound UA-5.

## 2. Materials and Methods

### 2.1. General Procedure

Chromatographic purifications were performed by column chromatography using 0.06–0.20 mm silica gel. NMR spectra were measured with a JEOL JNM-ECA 300/600 instrument (JEOL Ltd, Tokyo, Japan). A Bruker Esquire-LC spectrometer (Bruker, Fallanden, Switzerland) was employed to measure electrospray ionization mass spectrometry (ESI-MS). TEM was performed using a Tecnai Spiri 120 KV instrument (FEI, Hillsboro, OR, USA). Rheological properties were measured by a Physica MCR301 rotary rheometer (Anton Paar, Germany) at room temperature.

Triethylamine (Et<sub>3</sub>N), benzoyl chloride, toluene, chlorobenzene, *o*-dichlorobenzene, bromobenzene and DMF were purchased from Beijing Chemical Plant (analytical purity). All solid samples requiring drying were vacuum-dried for 5–10 h before use.

*p*-phenylenediamine, 1-ethyl-3-(dimethylaminopropyl) carbonyl diimide hydrochloride (EDCI), trifluoroacetic acid (TFA) and isophthaloyl dichloride were purchased from J&K Scientific Co., Ltd. (Beijing, China).

## 2.2. Synthesis

**Compound UA-1:** Initially, 5.0 g (10.4 mmol) of ursolic acid was dissolved in *N,N*-Dimethylformamide (DMF) (70 mL). Then, 1.6 g  $K_2CO_3$  (11.5 mmol) and 1.4 mL  $CH_3I$  (28 mmol) were added successively. The mixture was stirred for 24 h at room temperature. Then the mixture was poured into water and the resulting suspension was filtrated to give **UA-1** (solid, 3.9 g, 77%). ESI-MS (+)  $m/z$ : 493.3  $[M + Na]^+$ .  $^1H$  NMR ( $CDCl_3$ , 600 MHz):  $\delta$  5.24 (t, 1H,  $J = 6.8$  Hz), 3.60 (s, 3H), 3.20 (dd, 1H,  $J_1 = 20.6$  Hz,  $J_2 = 11.0$  Hz), 1.07, 0.98, 0.95, 0.91, 0.85, 0.77, 0.73, ( $7 \times s$ ,  $7 \times 3H$ , 23, 24, 25, 26, 27, 29, 30- $CH_3$ ).  $^{13}C$  NMR ( $CDCl_3$ , 150 MHz):  $\delta$  178.05 (28-C), 138.10 (13-C), 125.53 (12-C), 77.42 (3-C), 55.17, 52.84, 51.43, 48.05, 47.52, 41.96, 39.44, 39.01, 38.83, 38.72, 38.57, 36.93, 36.61, 32.93, 30.62, 28.11, 27.99, 27.19, 24.19, 23.58, 23.27, 21.17, 18.28, 17.01, 16.88, 15.59, 15.41.

**Compound UA-2:** To the solution of 220 mg (2.2 mmol) of succinic anhydride and 4-dimethylaminopyridine (DMAP) (15 mg) in 50 mL of pyridine (Pyr), 1.0 g (2.12 mmol) of **UA-1** was added. The reaction solution was stirred at 80 °C for 20 h. Then, the mixture was cooled to room temperature and poured in to 100 mL of water. After that, the solution was extracted with dichloromethane and the organic phase was washed with water and brine. It was then dried by  $MgSO_4$  and the solid was filtered out. The obtained liquid was evaporated and the solids were purified by column chromatography ( $CH_2Cl_2:CH_3OH = 50:1$ ) forming **UA-2** as a yellow solid (1.05 g, 87%). ESI-MS (−)  $m/z$ : 570.7  $[M-H]^{-1}$ .  $^1H$  NMR ( $CDCl_3$ , 600 MHz):  $\delta$  5.23 (t, 1H,  $J = 6.2$  Hz), 4.52 (t, 1H,  $J = 14.4$  Hz), 3.61 (s, 3H), 1.31, 1.06, 0.93, 0.86, 0.83, 0.83, 0.78 ( $7 \times s$ ,  $7 \times 3H \times 2$ , 23, 24, 25, 26, 27, 28, 30- $CH_3$ ).  $^{13}C$  NMR ( $CDCl_3$ , 200 MHz):  $\delta$  178.16, 177.09, 171.79, 138.10, 125.40, 81.48, 55.24, 52.79, 51.43, 48.03, 47.39, 41.91, 39.42, 38.97, 38.81, 38.17, 37.66, 36.78, 36.57, 32.82, 30.58, 29.26, 29.02, 28.84, 28.58, 27.94, 24.15, 23.40, 23.24, 21.14, 18.13, 17.02, 16.83, 16.69, 15.42.

**Compound UA-3:** 1-(3-Dimethylaminopropyl)-3-ethylcarbodiimide Hydrochloride (EDCI) (1.03 mmol) and Boc protected *p*-phenylenediamine (215 mg) were added to the solution of 500 mg (0.88 mmol) of **UA-2** in 8 mL of dry  $CHCl_3$ . Then the reaction mixture was stirred for 32 h at room temperature. After that the mixture was washed with water (20 mL) and brine (20 mL) and dried by  $MgSO_4$ . The solid was filtered out and the obtained liquid was evaporated. The solid was purified by column chromatography (PE: $CH_3CO_2C_2H_5 = 4:1$ ) forming **UA-3** as a yellow solid (315 mg, 47%). ESI-MS (+)  $m/z$ : 784.0  $[M + Na]^+$ .  $^1H$  NMR (600 MHz,  $CDCl_3$ ):  $\delta$  7.75 (s, 1H), 7.37 (d, 2H,  $J = 11.0$  Hz), 7.27 (d, 2H,  $J = 11.0$  Hz), 6.54 (s, 1H), 5.23 (s, 1H), 4.51 (m, 1H), 3.59 (s, 3H), 1.48 (s, 9H), 1.21, 0.90, 0.88, 0.87, 0.82, 0.82, 0.69, ( $7 \times s$ ,  $7 \times 3H$ , 23, 24, 25, 26, 27, 29, 30- $CH_3$ ).  $^{13}C$  NMR (100 MHz,  $CDCl_3$ )  $\delta$ : 178.03, 172.84, 169.65, 152.86, 138.04, 134.48, 133.25, 125.36, 120.56, 119.15, 81.46, 81.21, 60.32, 55.19, 52.75, 51.37, 47.97, 47.35, 41.86, 39.38, 38.92, 38.76, 37.64, 36.73, 28.27, 28.00, 23.48, 21.08, 16.97, 16.78, 16.66, 15.36.

**Compound UA-4:** At 0 °C, 2.4 mL of trifluoroacetic acid (TFA) was added to the solution of 500 mg (0.66 mmol) of **UA-3** in 8 mL of  $CH_2Cl_2$ . The reaction mixture was stirred for 8 h at room temperature. Then the solution was washed with saturated  $NaHCO_3$ , water (30 mL) and brine (30 mL), then dried by  $MgSO_4$  and evaporated. To obtain a solid, this compound was further purified by column chromatography ( $CH_2Cl_2:CH_3OH = 100:1$ ), forming **UA-4** as a yellow solid (427 mg, 85%). ESI-MS (+)  $m/z$ : 661.5  $[M + H]^+$ .  $^1H$  NMR (600 MHz,  $CDCl_3$ ):  $\delta$  7.64 (s, 1H), 7.23 (s, 2H,  $J = 17.28$  Hz), 6.60 (d, 2H,  $J = 17.2$  Hz), 5.23 (s, 1H), 4.51 (m, 1H), 3.54 (s, 3H), 1.06, 0.94, 0.91, 0.86, 0.83, 0.83, 0.72 ( $7 \times s$ ,  $7 \times 3H$ , 23, 24, 25, 26, 27, 29, 30- $CH_3$ ).  $^{13}C$  NMR (200 MHz,  $CDCl_3$ )  $\delta$ : 178.04, 172.95, 169.50, 142.98, 138.08, 129.32, 125.38, 121.86, 115.34, 81.48, 55.21, 52.77, 51.41, 47.99, 47.38, 41.89, 39.40, 38.95, 38.78, 37.67, 36.76, 28.04, 23.72, 22.76, 23.51, 21.12, 17.00, 16.81, 16.70, 15.39.

**Compound UA-5:** First 200 mg (0.30 mmol) **UA-4** and  $Et_3N$  (55  $\mu$ L) were dissolved in 12 mL dry tetrahydrofuran (THF) and cooled to 0 °C. Then 35  $\mu$ L of (0.35 mmol) benzoyl chloride was added to the above solution. The reaction mixture was stirred for 2 h at 50 °C. After that the

solution was filtered and evaporated to obtain a solid product. Purification was conducted by silica gel column with  $\text{CH}_2\text{Cl}_2:\text{CH}_3\text{OH} = 40:1$  as the eluent to produce **UA-5** as a light yellow solid (195 mg, 85%). HRMS (High-Resolution Mass Spectrum) calculated for  $\text{C}_{48}\text{H}_{65}\text{N}_2\text{O}_6$ : 765.4843, found: 765.4835.  $^1\text{H}$  NMR (600 MHz,  $\text{CDCl}_3$ ):  $\delta$  8.38, 8.24 (2×s, 2H), 7.86 (d, 2H,  $J = 14.4$  Hz), 7.46–7.36 (m, 7H), 5.21 (s, 1H), 4.51 (m, 1H), 3.59 (s, 3H), 1.05, 0.93, 0.90, 0.85, 0.83, 0.83, 0.71 (7×s, 7×3H, 23, 24, 25, 26, 27, 29, 30- $\text{CH}_3$ ).  $^{13}\text{C}$  NMR (200 MHz,  $\text{CDCl}_3$ ):  $\delta$  178.09, 172.92, 170.00, 165.97, 138.07, 134.69, 134.56, 133.92, 131.69, 128.58, 127.17, 125.38, 121.53, 120.75, 81.54, 55.21, 52.77, 51.43, 48.01, 47.37, 41.89, 39.40, 38.95, 38.79, 37.67, 36.76, 28.06, 23.53, 23.21, 21.13, 17.01, 16.83, 16.72, 15.41.

### 3. Results and Discussion

The gelation behaviors of **UA-5** in solvents were measured by the method of “stable to the inversion of a tube” [30]. Certain amounts of **UA-5** and solvent were put into a sealed glass bottle and heated. Then, the mixture was treated with ultrasound and cooled to room temperature. Subsequently the bottle was inverted to observe if a gel had formed. The observed gelation behaviors are presented in Table 1. Transparent gel formations in some aromatic solvents such as chlorobenzene, bromobenzene and *o*-dichlorobenzene were observed (Figure 1) and they were all stable at room temperature for several days. The product was soluble in polar aprotic solvents like dimethylformamide (DMF), tetrahydrofuran (THF) and dimethyl sulfoxide (DMSO), and insoluble in some protonic solvents like methanol and water. In nonpolar solvents such as benzene and petroleum ether, it formed a precipitate state. Only the solvents with suitable polarity could be gelled by the gelators of **UA-5**. As the literature suggests, gelation formed due to a balance of good solubility and the aggregation of the gelators [31]. Mixed solvents were also tested. **UA-5** was soluble in chloroform, in which it formed a clear solution and turned into a transparent gel at room temperature after the gradual addition of toluene or *p*-xylene under sonication. In addition, the gelation property ( $T_{\text{gel}}$ ) indicating the required temperature for gel to break was affected by the volume proportions of the solvents.  $T_{\text{gel}}$  was tested and plotted as a function of volume proportions of toluene under the same gelator concentration. Obviously, the  $T_{\text{gel}}$  illustrating the thermal stability of the gel was the maximum at a volume ratio of 2:1 between toluene with chloroform (Figure 2). The ursolic acid derivatives (except **UA-5**) could not form organogel in the tested solvents, perhaps due to the insufficient hydrogen bonding and  $\pi$ - $\pi$  stacking.

**Table 1.** Gelation behaviors of **UA-5**.

Entry	Solvent	State <sup>a</sup>	MGC <sup>b</sup> (g/100 cm <sup>3</sup> )
1	chlorobenzene	G	1.8±0.1
2	bromobenzene	G	2.6±0.1
3	<i>o</i> -dichlorobenzene	G	1.0±0.1
4	chloroform/toluene(1/2)	G	0.8±0.1
5	chloroform/ <i>p</i> -xylene(1/2)	G	1.0±0.1

<sup>a</sup> G, gel; <sup>b</sup> MGC, minimum gelator concentration (g/100 cm<sup>3</sup>) at which the gel could be formed at 25 °C.



**Figure 1.** Gels in chloroform/toluene, chloroform/*p*-xylene, *o*-dichlorobenzene, bromobenzene, chlorobenzene (from left to right).

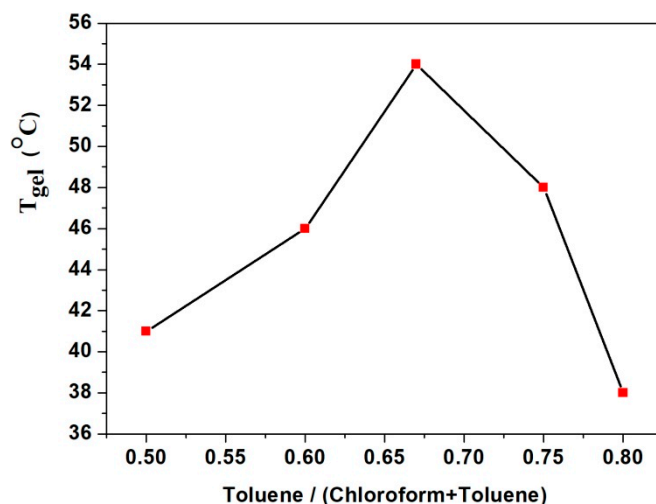


Figure 2. Plot of  $T_{gel}$  vs. percent volume of toluene.

Transmission electron microscopy (TEM) was employed to observe the morphology of supramolecular gels. As shown in Figure 3a, the xerogel in chlorobenzene presented a typical 3D fiber network structure with fiber diameters of about 100 nm. We should note that the nanofiber diameters in different solvent systems were different. Entangled nanofibers with a width of about 50 nm creating a closely packed 3D network could also be observed in the xerogel from chloroform and toluene above the minimum gelator concentration (MGC) (Figure 3b). Obviously, as the gel became more stable, it exhibited a thinner fibrous structure and closer entanglement, which was consistent with the stability in different solvents indicated by the MGC values. A reasonable explanation for this was that the close cross-linking network could immobilize more solvent molecules. Under the MGC, UA-5 could also self-assemble into fibers in chloroform induced by toluene, but these were too short to entangle together to form an organogel (Figure 3c).

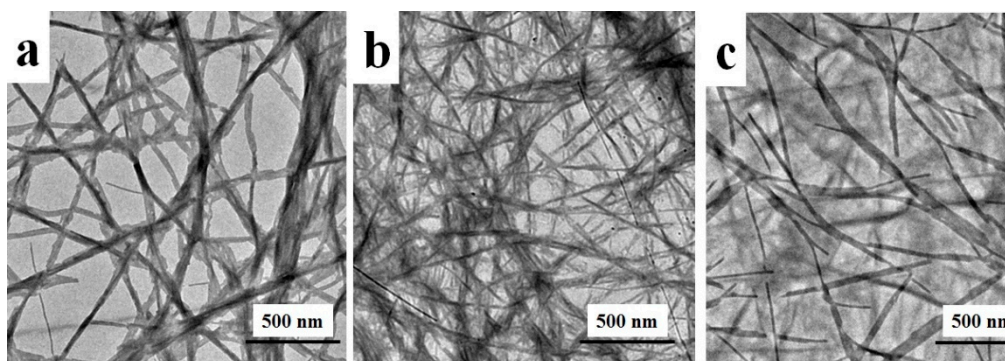


Figure 3. TEM images of gel in (a): chloroform ( $1.9 \text{ g}/100 \text{ cm}^3$ ); (b): chloroform/toluene = 1:2  $v/v$  ( $0.9 \text{ g}/100 \text{ cm}^3$ ); (c): chloroform/toluene = 1:2  $v/v$  ( $0.6 \text{ g}/100 \text{ cm}^3$ ).

Fourier-transform infrared spectra (FT-IR) and  $^1\text{H}$  NMR experiments were performed to infer the driving forces of the gel formation [32–34]. FT-IR spectra showed that in the gel state, the aliphatic C–H stretching vibration band of ursolic acid skeleton appeared at a lower wavenumber ( $2997 \text{ cm}^{-1}$ ) compared with that in the solid state ( $3006 \text{ cm}^{-1}$ ). It illustrated that the increased van der Waals interaction of aggregated gelators drive the gel formation. In addition, compared with the solid state, the NH bending (amide II) band shifted from  $1552 \text{ cm}^{-1}$  to  $1542 \text{ cm}^{-1}$  when the gel formed. In the solid state, the peak at  $1647 \text{ cm}^{-1}$  was assigned to the C=O stretching band (amide I) and benzene skeleton vibration, which split into two peaks at  $1644 \text{ cm}^{-1}$  and  $1675 \text{ cm}^{-1}$  in the gel (Figure 4). The above results revealed that hydrogen bonding between amide groups and  $\pi$ – $\pi$  interaction between benzene

rings promoted the formation of organogels. The variable temperature  $^1\text{H}$  NMR of UA-5 spectra in deuterated chloroform and toluene were performed to confirm the driving forces and the results are shown in Figure 5. As the temperature increased from 25 °C to 45 °C, the gel changed into a solution state gradually, while the amide protons and aromatic protons upfieldshifted gradually, implying that the  $\pi$ - $\pi$  interaction between the aromatic rings and hydrogen bonding played synergic roles for gel formation [15,17].

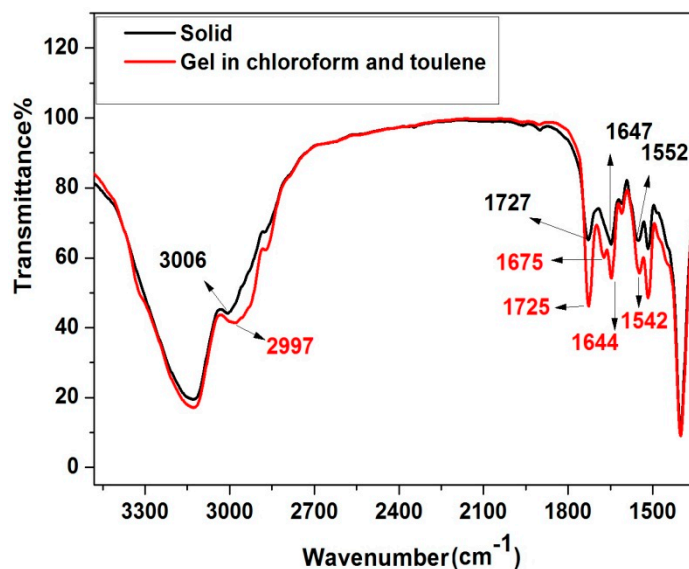


Figure 4. FT-IR spectra of UA-5 in gel state and solid state.

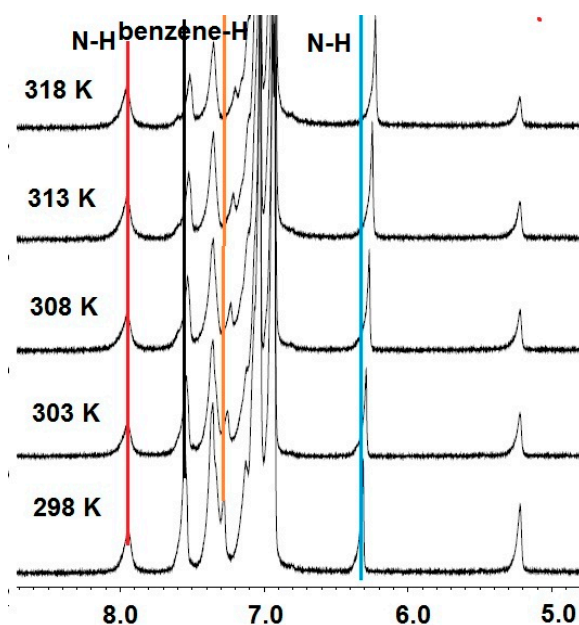
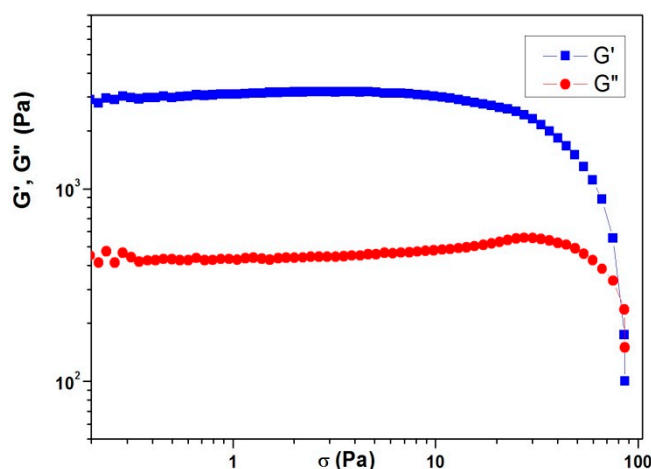


Figure 5.  $^1\text{H}$  NMR spectra of UA-5 in chloroform and toluene (1:2  $v/v$ ) mixture at different temperatures.

To explore the mechanical properties of the gel, rheological measurement was conducted on the gel in *o*-dichlorobenzene, in which self-assembly fibers yield a cross-linked three dimensional network. The storage modulus  $G'$  and the loss modulus  $G''$  which characterized the viscoelastic behavior of the gels were measured as functions of shear stress at a constant frequency of 1.0 Hz at 25 °C. As shown in Figure 6, it exhibited a clear thixotropic property and the beginning  $G'$  was about seven times greater than  $G''$ , indicating the dominant elastic characteristic of this gel [35,36]. A sudden decrease in the

two values was observed above 86 Pa, indicating the breakup of the gel networks under high shearing force—in other words, an indication of a dominant fluidity characteristic.



**Figure 6.** Values (Pa) of  $G'$  and  $G''$  of the gel in *o*-dichlorobenzene ( $1.2 \text{ g}/100 \text{ cm}^3$ ) as functions of applied shear stress.

#### 4. Conclusions

Aromatic rings as functional groups were conjugated to ursolic acid and the derivative could self-assemble into a supramolecular gel based on intermolecular hydrogen bonding,  $\pi$ - $\pi$  stacking interaction as well as the aggregation property of the ursane-triterpenoid skeleton. Introducing functional groups at the A ring, providing non-covalent interactions, proved to be a feasible method to develop supramolecular self-assembly architecture from biocompatible ursolic acid. Moreover, this study expands the building block for self-assembly from natural product triterpenoids. The authors hope to contribute to the design of more functional molecules based on ursolic acid to form supramolecular self-assemblies in the future.

**Author Contributions:** Conceptualization, J.L. and Y.L.; methodology, J.H. and W.C.; validation, J.L., Y.L. and W.C.; formal analysis, J.H. and J.L.; writing—original draft preparation, J.L., J.H. and Y.L.; writing—review and editing, W.C.; visualization, J.L. and W.C.; supervision, Y.L.; project administration, W.C.; funding acquisition, J.L., Y.L. and W.C.

**Funding:** This research was funded by the Natural Science Foundation of Hebei Province (B2016209139), One Hundred Excellent Talents of Innovation in Hebei Provincial Universities (III) (No. SLRC2017049) and the National Natural Science Foundation of China (No. 51372068).

**Acknowledgments:** We thank Ju's group of Tsinghua University for the NMR measurement.

**Conflicts of Interest:** The authors declare no conflict of interest.

#### References

1. Steed, J.W. Supramolecular gel chemistry: Developments over the last decade. *Chem. Commun.* **2011**, *47*, 1379–1383. [[CrossRef](#)] [[PubMed](#)]
2. Tu, T.; Zhu, H. Recent Advance between Supramolecular Gels and Catalysis. *Chem. Asian. J.* **2018**, *13*, 712–729.
3. Buerkle, L.E.; Rowan, S.J. Supramolecular gels formed from multi-component low molecular weight species. *Chem. Soc. Rev.* **2012**, *41*, 6089–6102. [[CrossRef](#)] [[PubMed](#)]
4. Li, C.X.; Jin, Q.X.; Lv, K.; Zhang, L.; Liu, M.H. Water tuned the helical nanostructures and supramolecular chirality in organogels. *Chem. Commun.* **2014**, *50*, 3702–3705. [[CrossRef](#)] [[PubMed](#)]
5. Suthiwangcharoen, N.; Li, T.; Wu, L.; Reno, H.B.; Thompson, P.; Wang, Q. Facile co-assembly process to generate core-shell nanoparticles with functional protein corona. *Biomacromolecules* **2014**, *15*, 948–956. [[CrossRef](#)]

6. Gao, Y.X.; Hu, J.; Ju, Y. Supramolecular Self-Assembly Based on Natural Small Molecules. *Acta.Chim. Sinica*. **2016**, *74*, 312–329. [[CrossRef](#)]
7. Du, X.; Zhou, J.; Xu, B. Supramolecular hydrogels made of basic biological building blocks. *Chem. Asian J.* **2014**, *9*, 1446–1472. [[CrossRef](#)] [[PubMed](#)]
8. Nelli, S.R.; Chakravarthy, R.D.; Mohiuddin, M.; Lin, H.C. The role of amino acids on supramolecular co-assembly of naphthalenediimide–pyrene based hydrogelators. *RSC Adv.* **2018**, *8*, 14753–14759. [[CrossRef](#)]
9. Lu, J.; Ju, Y. Organogels Based on Natural Products. *Chin. J. Org. Chem.* **2013**, *33*, 469–482. [[CrossRef](#)]
10. Bag, B.G.; Majumdar, R.; Laguerre, M. Natural triterpenoids as renewable nanos. *Struct. Chem.* **2012**, *23*, 393–398. [[CrossRef](#)]
11. Bag, B.G.; Dinda, S.K.; Dey, P.P.; Mallia, V.A.; Weiss, R.G. Self-assembly of esters of arjunolic acid into fibrous networks and the properties of their organogels. *Langmuir* **2009**, *25*, 8663–8671. [[CrossRef](#)] [[PubMed](#)]
12. Bag, B.G.; Majumdar, R. Vesicular self-assembly of a natural triterpenoid arjunolic acid in aqueous medium: Study of entrapment properties and in situ generation of gel–gold nanoparticle hybrid material. *RSC Adv.* **2014**, *4*, 53327–53334. [[CrossRef](#)]
13. Bag, B.G.; Majumdar, R. Self-assembly of a renewable nano-sized triterpenoid 18 $\beta$ -glycyrrhetic acid. *RSC Adv.* **2012**, *2*, 8623–8626. [[CrossRef](#)]
14. Gao, Y.; Hao, J.; Wu, J.; Hu, J.; Ju, Y. Cooperative supramolecular helical assembly of a pyridinium-tailored methyl glycyrrhetate. *Soft Matter* **2016**, *12*, 8979–8982. [[CrossRef](#)]
15. Lu, J.R.; Hu, J.; Song, Y.; Ju, Y. A new dual-responsive organogel based on uracil-appended glycyrrhetic acid. *Org. Lett.* **2011**, *13*, 3372–3375. [[CrossRef](#)] [[PubMed](#)]
16. Lu, J.R.; Gao, Y.X.; Wu, J.D.; Ju, Y. Organogels of triterpenoid–tripeptide conjugates: Encapsulation of dye molecules and basicity increase associated with aggregation. *RSC Adv.* **2013**, *3*, 23548–23552. [[CrossRef](#)]
17. Lu, J.R.; Wu, J.D.; Ju, Y. Tuning the aggregation mode to induce different chiralities in organogels of mono- and bistriterpenoid derivatives and the preparation of gold nanoparticles for use as a template. *New J. Chem.* **2014**, *38*, 6050–6056. [[CrossRef](#)]
18. Saha, A.; Adamcik, J.; Bolisetty, S.; Handschin, S.; Mezzenga, R. Fibrillar Networks of Glycyrrhizic Acid for Hybrid Nanomaterials with Catalytic Features. *Angew. Chem. Int. Ed.* **2015**, *54*, 5408–5412. [[CrossRef](#)] [[PubMed](#)]
19. Bag, B.G.; Dash, S.S. First self-assembly study of betulinic acid, a renewable nano-sized, 6-6-6-6-5 pentacyclic monohydroxy triterpenic acid. *Nanoscale* **2011**, *3*, 4564–4566. [[CrossRef](#)] [[PubMed](#)]
20. Bag, B.G.; Dash, S.S. Hierarchical Self-Assembly of a Renewable Nanosized Pentacyclic Dihydroxy-triterpenoid Betulin Yielding Flower-Like Architectures. *Langmuir* **2015**, *31*, 13664–13672. [[CrossRef](#)] [[PubMed](#)]
21. Gao, Y.; Hao, J.; Wu, J.; Zhang, X.; Hu, J.; Ju, Y. Solvent-Directed Assembly of a Pyridinium-Tailored Methyl Oleanolate Amphiphile: Stepwise Growth of Microrods and Nanofibers. *Langmuir* **2016**, *32*, 1685–1692. [[CrossRef](#)] [[PubMed](#)]
22. Lu, J.R.; Hu, J.; Liu, C.L.; Gao, H.X.; Ju, Y. Water-induced gel formation of an oleanolic acid–adenine conjugate and the effects of uracil derivative on the gel stability. *Soft Matter* **2012**, *8*, 9576–9580. [[CrossRef](#)]
23. Lu, J.R.; Ju, Y. Supramolecular Gels Based on Natural Product-Triterpenoids. *Process. Chem.* **2016**, *28*, 260–268.
24. Ikeda, Y.; Murakami, A.; Ohigashi, H. Ursolic acid: An anti- and pro-inflammatory triterpenoid. *Mol. Nutr. Food. Res.* **2010**, *52*, 26–42. [[CrossRef](#)] [[PubMed](#)]
25. Dar, B.A.; Lone, A.M.; Shah, W.A.; Qurishi, M.A. Synthesis and screening of ursolic acid-benzylidene derivatives as potential anti-cancer agents. *Eur. J. Med. Chem.* **2016**, *111*, 26–32. [[CrossRef](#)] [[PubMed](#)]
26. Zhang, C.; Xu, S.H.; Ma, B.L.; Wang, W.W.; Yu, B.Y.; Zhang, J. New derivatives of ursolic acid through the biotransformation by *Bacillus megaterium* CGMCC 1.1741 as inhibitors on nitric oxide production. *Bioorg. Med. Chem. Lett.* **2017**, *27*, 2575–2578. [[CrossRef](#)] [[PubMed](#)]
27. Lu, J.R.; Wu, X.N.; Chen, H.P.; Liang, Y.H. First Organogelation Study of Ursolic Acid, a Natural Ursane Triterpenoid. *Chem. Lett.* **2016**, *45*, 860–862.
28. Ma, M.; Kuang, Y.; Gao, Y.; Zhang, Y.; Gao, P.; Xu, B. Aromatic-aromatic interactions induce the self-assembly of penta peptidic derivatives in water to form nanofibers and supramolecular hydrogels. *J. Am. Chem. Soc.* **2010**, *132*, 2719–2728. [[CrossRef](#)]
29. Shin, S.; Lim, S.; Kim, Y.; Kim, T.; Choi, T.L.; Lee, M. Supramolecular Switching between Flat Sheets and Helical Tubules Triggered by Coordination Interaction. *J. Am. Chem. Soc.* **2013**, *135*, 2156–2159. [[CrossRef](#)]



30. Velazquez, D.G.; Diaz, D.D.; Ravelo, A.G.; Marrero-Tellado, J.J. Hunter's Oligoamide: A Functional C2-Symmetric Molecule with Unusual Topology for Selective Organic Gel Formation. *Eur. J. Org. Chem.* **2007**, *2007*, 1841–1845. [[CrossRef](#)]
31. Niu, L.; Song, J.; Li, J.; Tai, N.; Lu, M.; Fan, K. Solvent effects on the gelation performance of melamine and 2-ethylhexylphosphoric acid mono-2-ethylhexyl ester in water–organic mixtures. *Soft Matter* **2013**, *9*, 7780–7786. [[CrossRef](#)]
32. Li, Y.; Gao, Y.; Wang, B.; Hao, J.; Hu, J.; Ju, Y. Natural Triterpenoid- and Oligo(Ethylene Glycol)-Pendant-Containing Block and Random Copolymers: Aggregation and pH-Controlled Release. *Chem. Asian. J.* **2018**, *13*, 2723–2729. [[CrossRef](#)] [[PubMed](#)]
33. Kar, H.D.; Gehrig, W.; Laquai, F.; Ghosh, S. J-aggregation, its impact on excited state dynamics and unique solvent effects on macroscopic assembly of a core-substituted naphthalenediimide. *Nanoscale* **2015**, *7*, 6729–6736. [[CrossRef](#)] [[PubMed](#)]
34. Gao, Y.; Hao, J.; Yan, Q.; Du, F.; Ju, Y.; Hu, J. A Natural Triterpenoid-Tailored Phosphate: In Situ Reduction of Heavy Metals Spontaneously to Generate Electrochemical Hybrid Gels. *Acs Appl. Mater. Interfaces* **2018**, *10*, 17352–17358. [[CrossRef](#)] [[PubMed](#)]
35. Dyakonova, M.A.; Stavrouli, N.; Popescu, M.T.; Kyriakos, K.; Grillo, I.; Philipp, M.; Jaksch, S.; Tsitsilianis, C.; Papadakis, C.M. Physical Hydrogels via Charge Driven Self-Organization of a TriblockPolyampholyte—Rheological and Structural Investigations. *Macromolecules* **2014**, *47*, 7561–7572. [[CrossRef](#)]
36. Kirilov, P.; Palomo, M.C. Colloidal dispersions of gelled nanoparticles (GLN): Concept and potential applications. *Gels* **2017**, *3*, 33–46.



© 2019 by the authors. Licensee MDPI, Basel, Switzerland. This article is an open access article distributed under the terms and conditions of the Creative Commons Attribution (CC BY) license (<http://creativecommons.org/licenses/by/4.0/>).